Dry Soil-Aggregate Stability: Energy-Based Index[1]

E. L. SKIDMORE AND D. H. POWERS[2]

ABSTRACT

Most methods used to estimate aggregate stability apply an unmeasured force, or a measured force without knowledge of transfer, to a single or a group of aggregates. A technique is needed to estimate aggregate stability based on quantitative transfer of energy. This paper presents an energy-based procedure for evaluating dry-aggregate stability. Soil aggregates were crushed by diametrically loading them between parallel plates. The energy of crushing was determined by integrating the area under the force against distance curve. The aggregate-surface area after comminution was calculated from aggregate-size distribution and aggregate density; the aggregates were assumed to be spherical. The results are expressed as energy per unit of surface area, joules per meter squared (J/m^2). Example values obtained from field-sampled aggregates for several soil series ranged from 3.7 ± 0.7 for Hotlake silt loam (coarse-silty, mixed, mesic Aquic Haploxerolls) to 43.9 ± 7.5 for Bearden silt loam (fine-silty, frigid Aeric Calciaquolls). The wide range of aggregate stabilities among different soils made it possible to distinguish among them even though variability among aggregates of the same soil was relatively large. The results were relatively insensitive to initial aggregate size but sensitive to crushing end point.

Additional Index Words: **mechanical stability, soil structure, rupture stress.**

Skidmore, E. L., and D. H. Powers. 1982. Dry soil-aggregate stability: energy-based index. Soil Sci. Soc. Am. J. 46:1274–1279.

A MAJOR PORTION of mineral soils consist of solid particles ranging in size from <0.1 to >1,000 µm. These primary individual particles associate together in various arrangements to form secondary or compound particles or aggregates. The particles are cemented by inorganic and organic bonding agents.

The size distribution and stability of these aggregates influence greatly the soils' physical properties and the processes that occur in the soil. Additionally, the size and stability of aggregates determine the soil's susceptibility to wind and water erosion. Aggregates between 0.05 and 0.50 mm in diameter are most easily transported by wind (Chepil, 1958). Aggregates larger than 0.84 mm are resistant to wind transport. The 0.05- to 0.25-mm size range dominates water sediments from high sand soils, and aggregates ranging in size from 0.02 to 0.20 mm are most erodible from high silt and clay soils (Young, 1980).

Aggregate size is important in determining the dimensions of pore space in cultivated soils. The size of the pores in turn affects the movement and distribution of water and air (major factors affecting plant growth) in the soil.

Many forces operating in the soil tend to cause a change in aggregate-size distribution. Aggregates may break into smaller units or combine into larger units by such actions as wetting and drying, rainfall impact, freezing and thawing, animal and machine traffic, abrasion from saltating particles, and tillage.

The resistance of soil aggregates to breakdown from physical forces is a measure of coherence or strength of cementation between or within the particles or soil aggregates. In the dry state, this resistance has been referred to as dry-aggregate stability or mechanical stability.

Several procedures have been used to evaluate dry-aggregate stability. Chepil (1953) determined a relative measure of coherence or strength of cementation between and within the soil aggregates in a dry state by rotary sieving and dividing the weight of soil material remaining on the sieve after sieving by the weight before sieving.

Chepil (1951) also determined stability against collision. A 500-g soil sample obtained from the field and dried was sieved, and the portion retained on a 0.42-mm sieve was placed in a metal cylinder 91.4 cm in length and 10.2 cm in diameter. The cylinder was inverted end-over-end 20 times. The aggregates were allowed to fall and strike the bottom on each inversion. The soil was then rotary sieved. The stability was expressed as percentage of the original weight of the soil retained on the 0.42-mm sieve (Chepil, 1951).

Toogood (1978) used air-dried samples of aggregates 1 to 2 mm in diameter for estimating dry stability. A 5-g sample of the aggregates was sieved vigorously on a 1-mm sieve for 1 min; the sample was weighed, then sieved vigorously for 4 min. The weight of sample remaining after 5 min, expressed as a percentage of the weight remaining after 1 min, indicated the stability of the dry aggregates.

Recognizing the desirability of knowing the work required to subdivide aggregates into smaller units, Marshall and Quirk (1950) used a drop-shatter method to determine the stability of natural aggregates. Air-dry samples were shattered by dropping them onto a concrete floor from various heights. The kinetic energy was dissipated by impact with the hard surface. The small amount of energy lost to heat evolution and rebound was neglected. Others (Grossman et al., 1959; Farrell et al., 1967; Gill and McCreery, 1960) have used the drop-shatter technique to establish the relationship between the energy imparted to the soil and the degree of fragmentation.

Rittinger, cited by Lowrison (1974), suggested that the energy consumed in size reduction of solids was proportional to the new surface area produced. Aggregate stability depends on the number and strength of bonds holding particles together. Logically, the work required to break those bonds and thus reduce aggregate size and create new external surface area would also be a measure of the stability of those aggregates.

The purpose of this study was to develop and evaluate a method for measuring dry-aggregate stability

---

[1] Contribution from the ARS–USDA, in cooperation with the Kansas Agricultural Experiment Station. Department of Agronomy Contribution 81-396-J. Received 17 Nov. 1981. Approved 30 Aug. 1982.

[2] Soil Scientist, ARS–USDA, and Research Assistant, Agronomy Department, respectively, Kansas State University, Manhattan, KS 66506.

[3] Trade and company names are included for the benefit of the reader and do not imply endorsement or preferential treatment of the product listed by the USDA.

based on the energy required to create new aggregate-surface area.

METHODS

Air-dry aggregates which had passed through a 19.1-mm (3/4 in) sieve and collected on a 12.7-mm (1/2 in) sieve were crushed by placing them individually on the compression table on the 0- to 100-kg load cell and then moving the crosshead of an Instron Model 1125 Universal Testing Instrument[3] 10 mm/min until the clod was crushed between the load cell compression table and anvil.

The crushed aggregate was sieved into 13 size divisions (<0.038, 0.038 to 0.053, 0.053 to 0.074, 0.074 to 0.106, 0.106 to 0.25, 0.25 to 0.50, 0.50 to 1.00, 1.00 to 2.00, 2.00 to 2.83, 2.83 to 3.36, 3.36 to 4.76, 4.76 to 6.35, and >6.35 mm). The crushed sample was placed on the top of the largest sieve of a nest of flat sieves ranging in size from 0.106 to 6.35 mm and shaken 10 s with a Tyler Portable Sieve Shaker, Model TX-24.[3] The material that passed through the 0.106-mm sieve was separated into the <0.106-mm size fractions by sieving 2 min with an Allen-Bradley Sonic Sifter, Model L3PF.[3]

The external surface area generated by crushing was approximated as follows: The aggregate surface area, A, in a soil mass, m_s, is the area per aggregate times the number of aggregates. The area of a spherical aggregate with diameter, d, is

$$A_p = \pi d^2. \quad [1]$$

The number of aggregates, n_p, in a given mass of soil is

$$n_p = 6m_s/\rho\pi d^3, \quad [2]$$

where ρ and d are bulk aggregate density and diameter, respectively. The surface area, A_s, of a group of spherical aggregates with diameter, d, in a soil mass is found by combining Eq. [1] and Eq. [2]:

$$A_s = 6m_s/\rho d. \quad [3]$$

By using Eq. [3] for all 13 aggregate size groups, we obtained total aggregate surface area of the crushed sample,

$$A_t = \frac{6}{\rho}\sum_{i=1}^{13} m_i/d_i, \quad [4]$$

where d_i is midrange diameter of aggregate size group and m_i is the mass of that fraction. The bulk density, ρ, of large (>20 mm) aggregates was determined similar to the method of Blake (1965), except that we used kerosene to saturate the aggregates and as the known-density liquid. The bulk density thus determined was used in Eq. [4]. By dividing the results of Eq. [4] by the mass of the initial aggregate, we obtained the newly exposed surface area per unit mass of soil.

We also approximated the external surface area generated by crushing based on the assumption that the resulting aggregates were prolate spheroids. A prolate spheroid is formed by the rotation of an ellipse about its major axis.

The surface area of a prolate spheroid is given by

$$A_e = 2\pi b^2\left(1 + \frac{a}{b\varepsilon}\sin^{-1}\varepsilon\right), \quad [5]$$

where a and b are major and minor semiaxes, respectively; ε is eccentricity and defined by

$$\varepsilon = \sqrt{a^2 - b^2}/a. \quad [6]$$

If the mass of soil aggregates were constituted by spheroids, then the number would be found by dividing the mass of the sample by the mass of each spheriod, with major and minor semiaxis of a and b, respectively. That is given by

$$N_e = 3m_s/4\pi ab^2\rho. \quad [7]$$

The number of aggregates in the sample times the surface area of each aggregate gives the surface of the sample. Equations [5] and [7] combine to give

$$A_e = \frac{3m_s}{2\rho a}\left(1 + \frac{a}{b\varepsilon}\sin^{-1}\varepsilon\right), \quad [8]$$

where A_e is the surface area of a group of spheroidal aggregates of mass m_s, density ρ, eccentricity ε, and major and minor semiaxes a and b, respectively.

The ratio of computed surface areas of aggregate spheroids and spheres of the same density and total mass is found by dividing Eq. [8] by Eq. [3]:

$$A_e/A_s = \frac{d}{4a}\left(1 + \frac{a}{b\varepsilon}\sin^{-1}\varepsilon\right), \quad [9]$$

where d is sphere diameter midpoint between separating sieves; a, b, and ε are as defined previously.

We examined 20 or more aggregates in each of the different size ranges of the Reading soil and computed A_e/A_s by Eq. [9].

Particles from each size range were scattered onto a microscope slide and examined with a Bausch and Lomb Sterozoom 7 1.0x through 7.0x variable power pod microscope[3] with a 10x eye piece. A supplementary lens that doubles the magnification was used to measure the smaller particles. A reticle (linear scale), installed in the microscope eyepiece, was calibrated with a stage micrometer slide. We measured the length or major axis and width or minor axis of individual particles. If the smallest possible rectangle were placed around a particle, the major and minor axes were length and width, respectively.

The work done in crushing the sample was determined by recording the force on the sample during crushing and the distance through which that force acted on a strip chart and then integrating the area under the curve. The force times distance area was integrated by cutting out the chart paper under the curve, weighing, and comparing that weight to weight of reference area of chart paper. By dividing the energy of crushing a clod by the clod's mass, we obtained energy per unit mass.

The work done in crushing the sample divided by the new surface area exposed gave energy per unit surface, J/m^2.

The rupture stress, RS, of aggregates was determined by Eq. [10],

$$\mathrm{RS} = \frac{(\mathrm{BL})\mathrm{g}}{1.209\,(m/\rho)^{2/3}}, \quad [10]$$

where BL is load at initial break, g is acceleration due to gravity, m is mass of aggregate, ρ is aggregate density, and 1.209 comes from $\pi(3/4\pi)^{2/3}$ in the calculation of cross-sectional area of sphere with mass, m, and density, ρ.

RESULTS AND DISCUSSION

An example of the load vs. crushing distance is shown in Fig. 1. As the parallel plates moved closer together, the pressure on the aggregate increased until the initial break and the aggregate began to shatter. Not always is the initial break so pronounced as illustrated in Fig. 1; sometimes it is more pronounced. But in all instances, one can see by the peaks and valleys where additional fracturing of the aggregate occurs. At some point fracturing ceases and compression of the fractured mass begins. That occurs when the load on the aggregate, as sensed by the load cell increases sharply and does not drop back but contin-

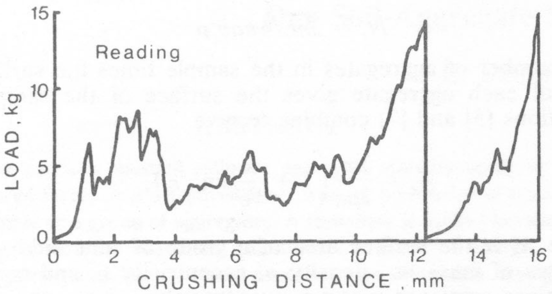

Fig. 1—Chart recording of load during crushing of Reading soil aggregates.

ues to increase, as depicted by the spike on the right side of Fig. 1. So as not to include energy of compression with the energy of crushing, we stopped crushing when the load was between the load at initial break and approximately twice the load at initial break, as detected by observing the chart recording.

To crush the aggregate more after that point has been reached, we reversed the direction of crosshead movement and spread the crushed sample out over the top of the load-cell compression table and repeated the crushing process. By then the initial aggregates already were small and distance of travel of the crosshead was short, as illustrated on the right portion of Fig. 1.

It appears in Fig. 1 that some compression occurred before crushing was stopped. In subsequent work, we have built a device to signal when the load is at 1.5 times (or some other programmable value) initial break load (Boyd et al., 1983).

We deliberately varied the degree of crushing on one sample of several aggregates by stopping the crosshead movement at different levels of crushing. The resulting crushing energy ranged from 36 to 351 J/kg of soil. The surface area after crushing was linearly related to the logarithm of the crushing energy (Fig. 2). Martin et al. (1926) found that by grinding sand in a ball mill, for a range of times, the additional surface produced bore a close linear relationship to the additional work done.

Lowrison (1974) suggested that there might be a relationship between the energy required to break material and the surface created in the breaking process, but that relationship would only be manifest if the energy consumed in creating a new surface could be measured separately, and doing that would be difficult. A plastic material will consume energy in changing shape, a shape it will retain without creating significant new surface. As fractured particles group together between the parallel plates, they give confining support to each other, and some energy is consumed in strain and heat.

For soil aggregates not so brittle as the sands of Martin et al. (1926), crushing breaks the most easily broken bonds first with a relatively small expenditure of energy. As the aggregate continues to be crushed, it takes increasingly more energy to further subdivide it. That could mean that not only are small aggregates more strongly bonded than are larger aggregates, but that a larger portion of the total work done is actually used in the comminution process as the particles get smaller.

Aggregate-size distribution of soil aggregates after crushing (Fig. 3) followed the same relationship as particle-size distribution of solid particles after comminution (Lowrison, 1974). On logarithm scales, both have a linear relationship between percentage passing a particular sieve size (accumulated frequency) and sieve size. The Monona and Bearden soils had 90.7 and 72.7%, respectively, of their total mass in the silt-plus clay-size fraction, and <10% of their crushed mass passed through the 0.05-mm sieve. That suggests that crushing did not reduce a large portion of the compound-particle aggregates to primary particles. In the case of coarse-textured soils, when a large portion of the primary particles are larger than 0.05 mm, a larger portion of the resulting aggregates would actually be primary particles. Currie (1966) proposed a method to evaluate change in porosity caused by interaction of aggregates and primary particles. In some preliminary results, we found a nonlinear relationship in a plot similar to that in Fig. 3.

Data of Fig. 3 illustrate that although only a small portion (15% or less) of the total mass was composed of aggregates smaller than 0.1 mm in diameter, a large

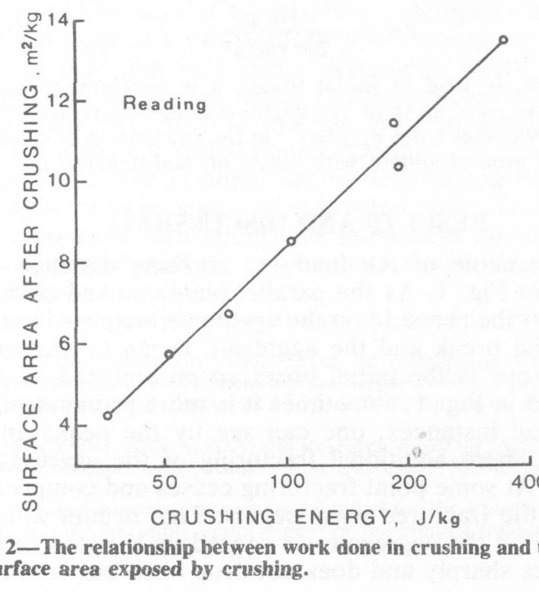

Fig. 2—The relationship between work done in crushing and the new surface area exposed by crushing.

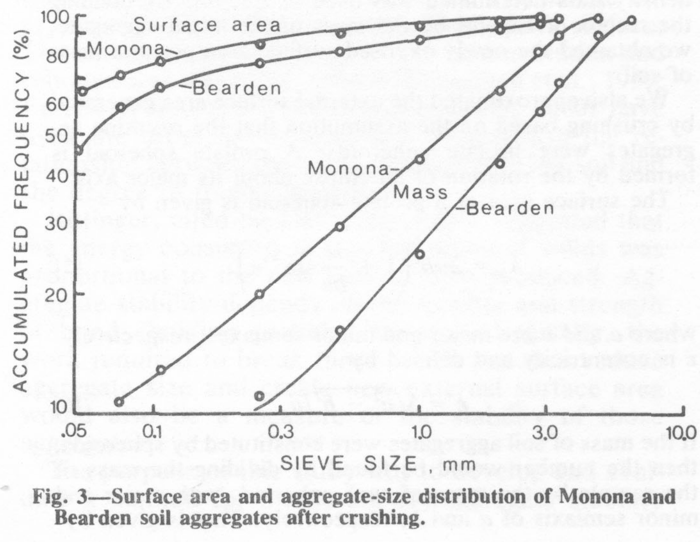

Fig. 3—Surface area and aggregate-size distribution of Monona and Bearden soil aggregates after crushing.

portion (60 to 80%) of the total surface area was associated with aggregates smaller than 0.1 mm. That necessitated careful sieving of the smaller size fractions for accurate surface-area determinations. Because it is more difficult to determine small- than large-size fractions, we had hoped we could combine some into larger groups for surface-area determinations. However, we found significant differences in results by combining the sizes that were differentiated by sonic sifting.

To characterize the dry-aggregate stability of a soil sample, each sample should be crushed to approximately the same end point. We did that by crushing each aggregate so that no more than 5% of the sample was held on the 6.35-mm sieve and at least 5% was held on the 3.36- to 4.75-mm sieve. Dry-aggregate stability of individual aggregates of several different soils group as shown in Fig. 4. Differences in dry-aggregate stability were clearly distinguishable. Hotlake required only 0.43 J to create a square meter of new aggregate surface area; the Bearden required 44 J/m^2. Dry-aggregate stability of several soils, for both natural and fabricated aggregates, is shown in Table 1.

Fabricated aggregates were those that had been formed in the laboratory. Soil was crushed and passed through a 2-mm sieve, then poured through a funnel into an 8.6- by 6.0-cm cylinder, and compacted by dropping the cylinder and soil 100 times through a distance of 1 cm. The soil was soaked by capillarity and dried at 25°C. After drying, the soil cylinder was broken to produce small chunks of soil which we called fabricated aggregates. The aggregates so formed were not nearly as stable as the ones formed naturally in the field unless they were compressed as was the Monona.

We selected 10 aggregates, in different size groups, of the Reading, Keith, and Hotlake soils, and we determined their aggregate stability. The results (Fig. 5) showed that the aggregates from the stabler soils, Keith and Reading, were not influenced by initial aggregate mass between about 3 and 30 g. Aggregates of the more fragile Hotlake soil, however, appeared to have been influenced by size. The group of the Hotlake aggregates of the largest sizes was significantly stabler at the 5% level according to Duncan's New Multiple Range Test (Steel and Torrie, 1960).

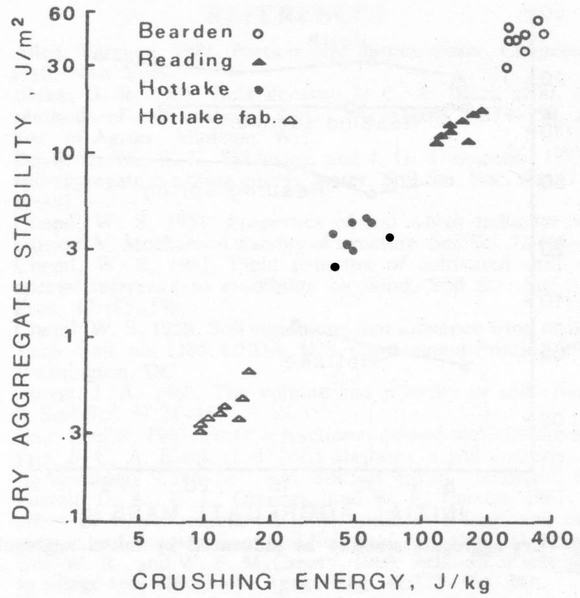

Fig. 4—Dry-aggregate stability of several soils.

The 3- to 10-g aggregate was found to be a convenient size range for crushing and sieving.

The influence of loading rate was evaluated by crushing 10 aggregates (3 to 7 g) of the Reading soil at each of the following speeds: 0.5, 2, 10, 50, and 200 mm/min. The mean and standard deviation aggregate stability index for each of those speeds were 14.9 ± 2.8, 17.2 ± 3.1, 13.7 ± 2.3, 15.3 ± 2.2, and 18.9 ± 7.0 J/m^2, respectively. None was significantly different from each other according to Duncan's New Multiple Range Test (Steel and Torrie, 1960) at either the 1 or 5% level.

The aggregate stability data in Table 1 were calculated based on the assumption that the aggregates after crushing were spheres, and Eq. [4] was used to calculate surface area. Had we assumed another shape, we would have gotten a slightly different answer.

Determination of a shape factor is a common problem in fine-particle technology (Allen, 1981; Kaye, 1981). It is difficult to mathematically describe a fine-particle surface except for simple geometric shapes as spheres, cubes, ellipsoids, and laminae. Fine particles do not conveniently come in one of those

Table 1—Soils used in the study of soil aggregate stability and some of their characteristics.

Series	Subgroup	Family	Sand	Silt	Clay	Textural class	Aggregates	Aggregate stability index, J/m^2
Bearden	Aeric Calciaquolls	Fine-silty, frigid	27.3	52.3	20.4	Silt loam	Natural	43.9 ± 7.5
Hotlake	Aquic Haploxerolls	Coarse-silty, mixed, mesic	10.2	67.0	22.8	Silt loam	Fabricated	0.41 ± 0.11
Hotlake	Aquic Haploxerolls	Coarse-silty, mixed, mesic	10.2	67.0	22.8	Silt loam	Natural	3.66 ± 0.73
Keith	Aridic Argiustolls	Fine-silty, mixed, mesic	12.6	57.9	29.6	Silty clay loam	Natural	20.3 ± 5.9
Monona	Typic Hapludolls	Fine-silty, mixed, mesic	9.3	76.6	14.1	Silt loam	Fabricated	0.44 ± 0.05
Monona	Typic Hapludolls	Fine-silty, mixed, mesic	9.3	76.6	14.1	Silt loam	Fabricated†	4.0 ± 1.1
Reading	Typic Arguidolls	Fine, mixed, mesic	11.1	60.6	28.3	Silty clay loam	Natural‡	5.0 ± 2.1
Reading	Typic Arguidolls	Fine, mixed, mesic	11.1	60.6	28.3	Silty clay loam	Natural§	13.7 ± 2.3
Richfield	Aridic Argiustolls	Fine, montmorillontic, mesic	17.7	61.4	20.9	Silt loam	Natural	2.47 ± 0.6
Ulysess	Aridic Haplustolls	Fine-silty, mixed, mesic	20.1	57.7	22.2	Silt loam	Natural	2.07 ± 0.75
Dalhart	Aridic Haplustalfs	Fine-loamy, mixed, mesic	74.1	13.7	12.2	Sandy loam	Natural	8.81 ± 2.0

† Compressed at 2.5 MPa with soil water matric potential at 100 J/kg.
‡ Spring sampled.
§ Fall sampled.

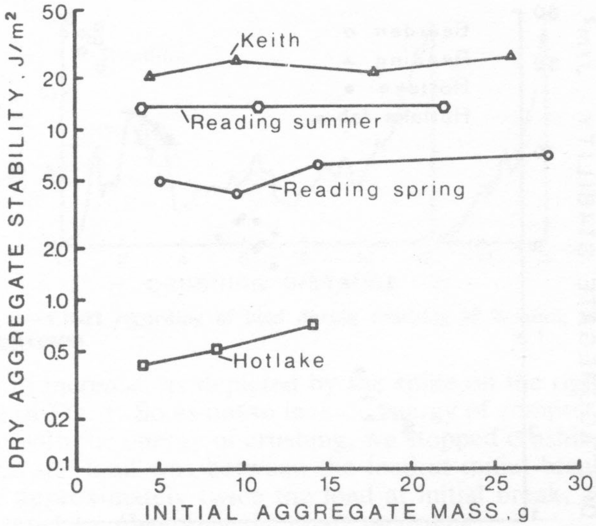

Fig. 5—Dry-aggregate stability as influenced by initial aggregate mass.

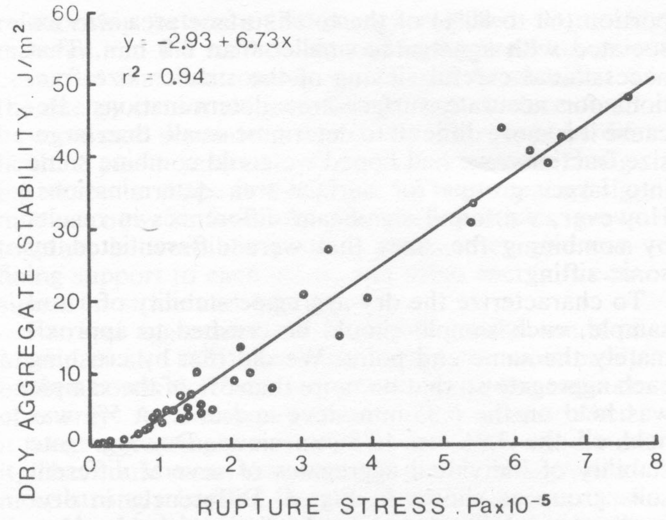

Fig. 6—Dry-aggregate stability estimated from rupture stress measurements. Soils used were Hotlake, Monona, Reading, Bearden, Keith, Richfield, and Ulysses, with aggregates ranging from approximately 4 to 25 g.

shapes, so we have to be satisfied with a limited description of a fine-particle dimension and structure based on either the geometric dimension or the functional behavior of the fine particle.

The A_e/A_s column in Table 2 shows a shape factor which we determined for each size group to convert to surface area based on the assumption that the aggregates were spheroids rather than spheres and have major and minor semiaxes as measured. The average shape factor for the 11 size ranges between <0.038 and >6.35 mm was 0.85 for the Reading soil.

One might expect the value of A_e/A_s to be >1.0 because the surface area of a spheroid is greater than the surface area of a sphere of the same volume, but the particles passing the sieves are larger than spheres of midrange sieve size diameter. The breadth of the particles was nearly always greater than the midrange sieve size, and the particle length was greater than the sieve opening. The particles tended to orient during sieving to pass the smallest possible sieve opening. Sahu (1965) also observed that sieves sort particles not only according to size but also according to shape, on the basis of the least cross-sectional area.

The unequal major and minor axes supports Rogowski's (1964) recommendation that aggregates should be considered as spheroids rather than spheres. Actually, the shape of the particles would likely be better described by ellipsoids than spheroids. However, measuring the third axis also adds another dimension to the difficulty of measuring.

In our calculations, Eq. [4], we assumed that the density of the aggregates in each size fraction was the same as the bulk density of a large aggregate of the same material before crushing. Rogowski (1964) and Rogowski and Kirkham (1967) found a range in density of aggregates from the plow layer of three Iowa soils. They separated the aggregates of those soils into density groups. Currie (1966) suggested that when the size of the aggregate is changed, there will be a change in the porosity of the sample. By considering that the pores exposed in crushing are lost, he predicted the decrease in aggregate porosity from crushing the aggregated material. One may also consider the exposed pores as being included in aggregate volume.

Dry-aggregate stability regressed against rupture stress (Fig. 6) showed an expected relationship. The more resistant an aggregate was to breaking, the more the energy that was required to comminute it. Although Fig. 6 is not intended to be a calibration curve, it shows that dry-aggregate stability can be estimated from measurements of rupture stress at initial break. In that no sieving or energy measurements are re-

Table 2—Shape factors, A_e/A_s, calculated from Eq. [9] for comparing the surface areas of spheroids and spheres of the same density and total mass.**

Sieve size range	Midpoint	Major semiaxis	Minor semiaxis	Eccentricity	A_e/A_s
mm				dimensionless	
<0.038	0.019	0.024 ± 0.005	0.015 ± 0.003	0.71 ± 0.19	0.59 ± 0.16
0.038–0.053	0.046	0.035 ± 0.007	0.024 ± 0.006	0.66 ± 0.22	0.88 ± 0.27 ab
0.053–0.075	0.064	0.055 ± 0.01	0.035 ± 0.005	0.73 ± 0.12	0.82 ± 0.12 b
0.075–0.125	0.100	0.09 ± 0.02	0.06 ± 0.01	0.65 ± 0.23	0.84 ± 0.29 ab
0.125–0.250	0.188	0.17 ± 0.035	0.105 ± 0.025	0.70 ± 0.22	0.88 ± 0.32 ab
0.250–0.50	0.375	0.325 ± 0.060	0.230 ± 0.045	0.685 ± 0.186	0.78 ± 0.14 b
0.50 –1.00	0.75	0.72 ± 0.14	0.46 ± 0.07	0.73 ± 0.13	0.75 ± 0.10 b
1.00 –2.00	1.50	1.18 ± 0.31	0.80 ± 0.19	0.66 ± 0.25	0.92 ± 0.24 ab
2.00 –2.80	2.42	1.61 ± 0.26	1.22 ± 0.17	0.59 ± 0.20	1.01 ± 0.16 a
2.80 –3.35	3.10	2.45 ± 0.36	1.75 ± 0.21	0.67 ± 0.12	0.82 ± 0.09 b
3.35 –4.75	4.06	2.99 ± 0.44	2.29 ± 0.29	0.60 ± 0.15	0.83 ± 0.10 ab
4.75 –6.35	5.56	4.16 ± 0.80	3.02 ± 0.33	0.63 ± 0.15	0.85 ± 0.08 ab

** Values followed by the same letter do not differ significantly at the 1% level.

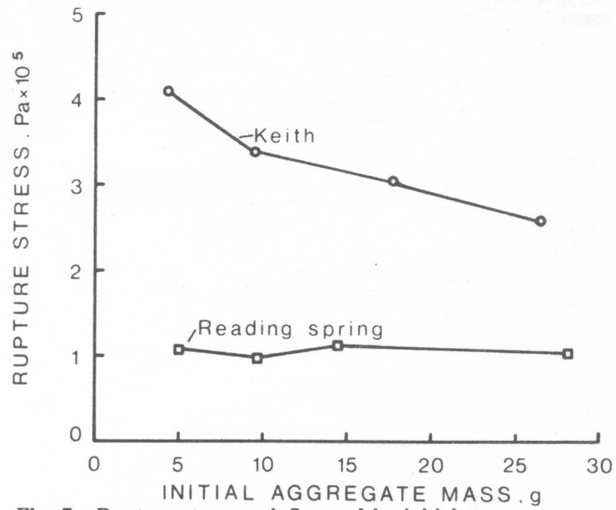

Fig. 7—Rupture stress as influenced by initial aggregate mass.

quired for rupture stress measurements, rupture stress data are easier to obtain than dry-aggregate stability data. However, we found that rupture stress appeared to be influenced more than crushing energy by initial aggregate mass (compare Fig. 5 and 7). Rogowski et al. (1968) also found rupture stress was influenced by initial aggregate size.

CONCLUSIONS

The dry-aggregate stability index reported here appears to be a reasonable approach to estimating dry-aggregate stability based on quantitative energy transfer. It can be used to estimate the energy a tillage implement must impart to a dry soil to produce a specified change in aggregate-size distribution. It can be used to measure crust strength, clod durability against multiple tillage operations, resistance of aggregates and crusts to abrasion from wind erosion, and also will be useful as a measurement tool in studying reasons for differences in aggregate stabilities.

Additional experience is needed to compare dry-aggregate stability index to field observations of wind erodibility, dry soil consistence, crust strength, and to develop a more simple and less expensive device to measure energy-based dry-aggregate stability index than what we used in this research.

REFERENCES

1. Allen, Terence. 1981. Particle size measurement. Chapman & Hall, New York.
2. Blake, G. R. 1965. Bulk density. *In* C. A. Black et al. (ed.) Methods of soil analysis, Part 1. Agronomy 9:374–390. Am. Soc. of Agron., Madison, Wis.
3. Boyd, D. W., E. L. Skidmore, and J. G. Thompson. 1983. A soil-aggregate crushing-energy meter. Soil Sci. Soc. Am. J. (in press).
4. Chepil, W. S. 1951. Properties of soil which influence wind erosion: V. Mechanical stability of structure. Soil Sci. 72:465–478.
5. Chepil, W. S. 1953. Field structure of cultivated soils with special reference to erodibility by wind. Soil Sci. Soc. Am. Proc. 17:185–190.
6. Chepil, W. S. 1958. Soil conditions that influence wind erosion. Tech. Bull. no. 1185, USDA. U.S. Government Printing Office, Washington, DC.
7. Currie, J. A. 1966. The volume and porosity of soil crumbs. J. Soil Sci. 17:24–35.
8. Day, Paul R. 1965. Particle fractionation and particle-size analysis. *In* C. A. Black et al. (ed.) Methods of soil analysis, Part 1. Agronomy 9:545–567. Am. Soc. of Agron., Madison, Wis.
9. Farrell, D. A., E. L. Greacen, and W. E. Larson. 1967. The effect of water content on axial strain in a loam soil under tension and compression. Soil Sci. Soc. Am. Proc. 31:445–450.
10. Gill, W. R., and W. F. McCreery. 1960. Relation of size of cut to tillage tool efficiency. Agric. Eng. 41:372–374, 381.
11. Grossman, R. B., J. B. Fehrenbacher, and A. H. Beavers. 1959. Fragipan soils of Illinois: I. General characterization and field relationships of Hosmer silt loam. Soil Sci. Soc. Am. Proc. 23:65–70.
12. Kaye, Brian H. 1981. Direct characterization of fine particles. John Wiley & Sons, New York.
13. Lowrison, G. C. 1974. Crushing and grinding: the size reduction of solid materials. Butterworth and Co., London, England.
14. Marshall, T. J., and J. P. Quirk. 1950. Stability of structural aggregates of dry soil. Aust. J. Agric. Res. 1:266–275.
15. Martin, G., E. A. Bowes, and F. B. Turner. 1926. Researches on the theory of fine grinding. Part III. Connection between the surface area produced and the work done in tube-mill grinding of quartz sand. Trans. Ceram. Soc. 25:63–81.
16. Rogowski, A. S. 1964. Strength of soil aggregates. Ph.D. Dissertation. Iowa State Univ., Univ. Microfilms, Ann Arbor, Mich. (Diss. Abstr. 65-3773).
17. Rogowski, A. S., and Don Kirkham. 1967. Strength of soil aggregates: influence of size, density, and clay and organic matter content. Med. Fac. Landbouww. Rijksuniv. Gent 41:85–100.
18. Rogowski, A. S., W. C. Moldenhauer, and Don Kirkham. 1968. Rupture parameters of soil aggregates. Soil Sci. Soc. Am. Proc. 32:720–724.
19. Sahu, Basanta K. 1965. Theory of sieving. J. Sediment. Petrol. 35:750–753.
20. Steel, R. G. D., and J. H. Torrie. 1960. Principles and procedures of statistics. McGraw Hill Book Co., Inc., New York.
21. Toogood, J. A. 1978. Relation of aggregate stability to property of Alberta soils. p. 211–215. *In* W. W. Emerson et al. (ed.) Modification of soil structure. John Wiley & Sons, New York.
22. Young, R. A. 1980. Characteristics of eroded sediment. Trans. Am. Soc. Agric. Eng. 23:1139–1142.